Classification and Segmentation of MRI Images of Brain Tumors Using Deep Learning and Hybrid Approach

Original Scientific Paper

Sugandha Singh
Department of Computer Science
Babasaheb Bhimrao Ambedkar University
Vidya Vihar, Rae Bareli Road, Lucknow (U.P.) 226025, INDIA
singhsugandha3@gmail.com

Vipin Saxena
Department of Computer Science
Babasaheb Bhimrao Ambedkar University
Vidya Vihar, Rae Bareli Road, Lucknow (U.P.) 226025, INDIA
vsax1@rediffmail.com

Abstract *– Manual prediction of brain tumors is a time-consuming and subjective task, reliant on radiologists' expertise, leading to potential inaccuracies. In response, this study proposes an automated solution utilizing a Convolutional Neural Network (CNN) for brain tumor classification, achieving an impressive accuracy of 98.89%. Following classification, a hybrid approach, integrating graph-based and threshold segmentation techniques, accurately locates the tumor region in magnetic resonance (MR) brain images across sagittal, coronal, and axial views. Comparative analysis with existing research papers validates the effectiveness of the proposed method, and similarity coefficients, including a Bfscore of 1 and a Jaccard similarity of 93.86%, attest to the high concordance between segmented images and ground truth.*

Keywords: *tumor images, graph-based approach, threshold segmentation, CNN, tumor identification, meningioma*

1. INTRODUCTION

Glioma, atypical meningioma, and schwannoma disease are among the most severe forms of brain tumor that pose a significant threat to human life. The primary brain tumor is estimated to affect 24,810 people by 2023 in the United States. In the early stage of a medical condition, patients may experience headaches. However, as time passes, the condition may progress, potentially leading to visual impairments [1]. Glioma is the most common primary brain tumor and the symptoms depend on the tumor's location, growth, and infiltration of tumors. Glioma symptoms can be quite severe. On the other hand, meningiomas are typically benign tumors that occur in adults. They are commonly found attached to the dura and arise from the meningothelial cell of the arachnoid. These tumors are rounded in shape with a well-defined dural base, which can lead to the compression of the underlying brain tissue. Meningiomas have two stages: atypical and anaplastic. Atypical meningiomas often exhibit a high rate of recurrence and more aggressive local growth. Atypical meningioma may require radiotherapy along with surgery. While most schwannomas within the cranial vault primarily occur at the cerebellopontine angle, where they are typically attached to the vestibular branch of the eight cranial nerves, the symptoms experienced by patients often include tinnitus and hearing loss. Early detection of these brain tumors is crucial for preventing further complications. Therefore, both classification and segmentation are critical factors in identifying brain tumors at an early stage [2].

Due to the abnormal and rapid growth of tumor tissues within the brain, it becomes imperative to accurately locate the position of the tumor that affects the brain cells. Worldwide, medical practitioners and radiologists are continually striving to diagnose brain tumors effectively. This is where MRI modalities play a crucial role in enhancing the accuracy of brain tumor diagnosis and identifying the affected areas. MRI is the dedicated imaging modality, a non-invasive technique widely used for detailed visualization of the brain's internal structures. The integration of artificial intelligence (AI) in MRI

analysis has become imperative due to the complex and voluminous nature of medical imaging data.

MRI generates high-dimensional and intricate datasets that pose challenges for efficient interpretation by human observers alone. The application of AI, particularly deep learning models like convolutional neural networks (CNNs), has shown promise in automating the analysis of MRI images. These models excel at discerning intricate patterns and features within the images, enabling more accurate and rapid identification of abnormalities, such as brain tumors.

Referring to existing literature, studies by Deb and Roy [3], and Ranjbarzadeh et al. [4] have explored the application of artificial intelligence (AI), specifically neural networks, for MRI image analysis. They emphasize the need for advanced computational techniques to handle the complexity of MRI data and enhance diagnostic accuracy. The introduction thus establishes the context of MRI as the chosen imaging modality and justifies the integration of AI to address the inherent challenges in its analysis, drawing on insights from relevant studies in the field. Noteworthy among these advancements is the work of Rehman et al. [5], which introduces a compelling strategy using an enhanced encoder-decoder network. 'BrainSeg-Net,' their novel approach, merits careful consideration in the broader landscape of medical image analysis.

To enhance the computational complexity and accuracy of brain tumor detection, a novel CNN based classification and segmentation method is employed. Samples of normal brain images and brain tumor images with glioma, atypical meningioma, and schwannoma, were collected from various hospitals as illustrated in Fig. 1 representing the transverse plane of both contrast and non-contrast MR images.

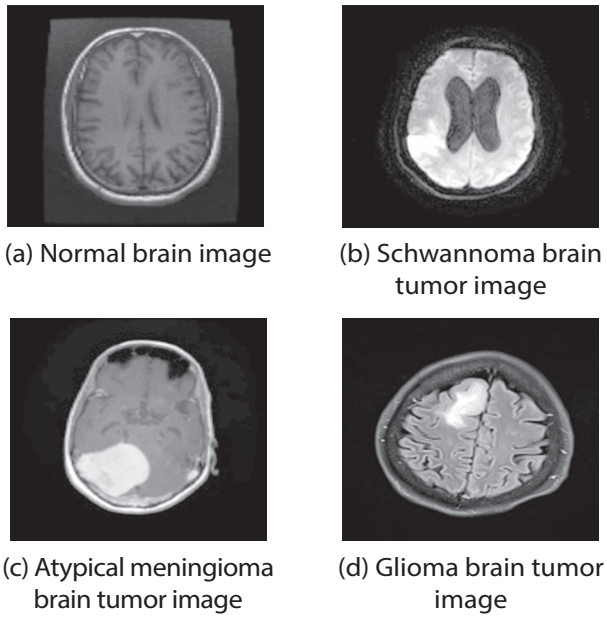

(a) Normal brain image

(b) Schwannoma brain tumor image

(c) Atypical meningioma brain tumor image

(d) Glioma brain tumor image

Fig. 1. Sample of (a) normal brain image and brain tumor images with (b) schwannoma, (c) atypical meningioma and (d) glioma

2. RELATED WORKS

In the references provided, the imaging modality used was primarily MRI (Magnetic Resonance Imaging). Specifically, Karayegen and Aksahin [6] utilized MRI for semantic segmentation to detect brain tumors using 3D imaging They compared ground truth with the segmented result. However, the classification error rate was not successfully minimized. Saleem et al. [7] utilized the MRI Brats 2018 dataset for 3D brain tumor segmentation and analyzed the segmentation model by applying interpretability technique to different tumor regions, including non-enhancing tumors, edema, and enhancing tumors. Khosravanian et al. [8] introduced a superpixels fuzzy clustering method with a multiscale morphological gradient reconstruction operation. They evaluated the method's performance on both synthetic data and the MR Brats 2017 dataset. However, a limitation of this paper is the use of single-modality MRI image fluid-attenuated inversion recovery (FLAIR) for tumor segmentation. Zhang et al. [9] introduced a multi-scale mesh aggregation network for MRI brain tumor image segmentation. One limitation of their approach is that the 2D network cannot fully leverage the details within the three spatial dimensions in 3D volume images. Lei et al. [10] employed a sparse constrained level set method to analyse brain tumor segmentation, implementing it using the MR Brats 2017 dataset. Their approach achieved higher accuracy compared to other methods. Shree and Kumar [11], utilized MR data extracted features using a grey-level co-occurrence matrix (GLCM) and applied discrete wavelet transform (DWT) with a region-growing segmentation method, achieving an accuracy of 98.02%. Mamatha et al. [12], introduced a graph theory based segmentation method in which a weighted directed graph is constructed. Each pixel in the image is represented as a nodes, and paths are obtained for the detection of MR brain tumors before the segmentation process. They applied pre-processing steps to enhance image quality and achieved favorable results. Balamurugan and Gnanamanoharan [13], present a novel approach employing a hybrid deep convolutional neural network (DCNN) with an enhanced LuNet classifier has been proposed. The primary goal is to precisely locate and classify MRI brain tumors as glioma or meningioma. The preprocessing stage involves the utilization of a laplacian gaussian filter (LOG), while a fuzzy c means with gaussian mixture model (FCM-GMM) algorithm is introduced for segmentation. The extended LuNet algorithm is then applied for data division, and VGG16 feature extraction yields thirteen categorical features. Hossain et al. [14], proposed method leverages lightweight deep learning models, namely MicrowaveSegNet, to achieve precise brain tumor segmentation, and BrainImageNet, for accurate image classification. The research integrates advanced computational techniques for efficient brain tumor analysis. The utilization of a portable sensor-based microwave imaging system adds a dimension of flexibility to the diagnostic process, showcasing the potential impact of this innovative methodology in the

field of medical imaging and brain tumor research. The proposed approach [15] combines adam sewing training based optimization with UNet++ (AdamSTBO+UNet++) for MRI brain tumor segmentation and adam salp water wave optimisation with the deep convolutional neural network (AdamSWO-DCNN) for classification. The introduction of AdamSTBO, an adaptation of the Adam optimizer integrated with the upgrade function of the sewing training based optimization (STBO) algorithm, signifies a distinctive advancement in optimization strategies. Ansari's [16], explores automated support systems for brain tumor detection using MRI, leveraging soft computing and machine learning algorithms. The study proposes a strategy utilizing a fuzzy clustering algorithm and a neural network system to identify brain tumor cells in their early stages. Ullah et al. [17] applied a statistical approach to enhance the image quality, to improve classification performance. For classification, they utilized discrete wavelet transform to extract features from MRI images and categorized them into malignant and benign tumor classes in deep neural networks. However, the limitations of this approach include its incompatibility with larger datasets and the longer execution time required. Amin et al. [18] applied a fusion technique using discrete wavelet transform (DWT) on MRI images. They employed a partial differential diffusion filter to remove noise and performed tumor segmentation using a global thresholding method. The segmented image was then passed to a proposed CNN model for classification into tumor and non-tumor regions. Their analysis revealed that fusion images provide superior results, and this method was extended to PET and CT images. However, a drawback was noted as the fusion images sometimes produced distorted images, which had an impact on the classification process.

While these studies do not directly resolve all the highlighted problems, each contributes valuable insights that could be leveraged to address the identified challenges. Techniques such as improved segmentation methods, utilization of multiple modalities, network enhancements, and preprocessing stages are all potential avenues to explore in minimizing classification errors and leveraging multi-modality imaging for more accurate tumor segmentation.

3. PROBLEM STATEMENT

The critical stage of brain tumor identification is a vital task to avoid severe brain issues. Several techniques have been developed to discover brain abnormalities through brain images in a precise manner. However, image classification and segmentation are the most challenging and essential tasks for medical images. Various segmentation techniques are applied to locating brain tumors, but they come with certain drawbacks and challenges. Which are listed below.

- The classification error rate in brain tumor segmentation needs to be minimized.
- The limitation of using single-modality MRI images for tumor segmentation.

These are the major challenges of different methods that motivate us to research on segmentation and classification. The paper addresses a suitable method to detect brain tumors more accurately and effectively.

4. MATERIAL AND METHOD

The aim of the research is to analyze radiologist's diagnoses using a deep learning model for classification and a hybrid approach for segmentation. The primary goal of the proposed method is to locate tumor-affected tissues in a more precise and efficient manner. The CNN approach is applied for the classification of tumor and no-tumor classes. The segmentation process partitions the tumor-affected tissues from healthy brain tissues, with practitioners performing this crucial step for clinical aids. The designed deep learning model, based on radiologist's assumptions, undergoes thorough analysis to achieve effective performance and accuracy surpassing existing approaches. The techniques are implemented and experimented with real MRI images collected from reputable hospitals are shown in Fig. 2.

1. In the pre-processing step, 2D MRI images are normalized to a scale of 1.0/255.0 using normalization techniques and resized to 224*224 to reduce computational complexity.
2. The 2D CNN model is applied to the trained images, and to perform classification into tumor and no-tumor.
3. After classification, the tumor region is located using a hybrid approach for tumor segmentation.
4. Evaluate the classification accuracy and segmentation similarity coefficients.

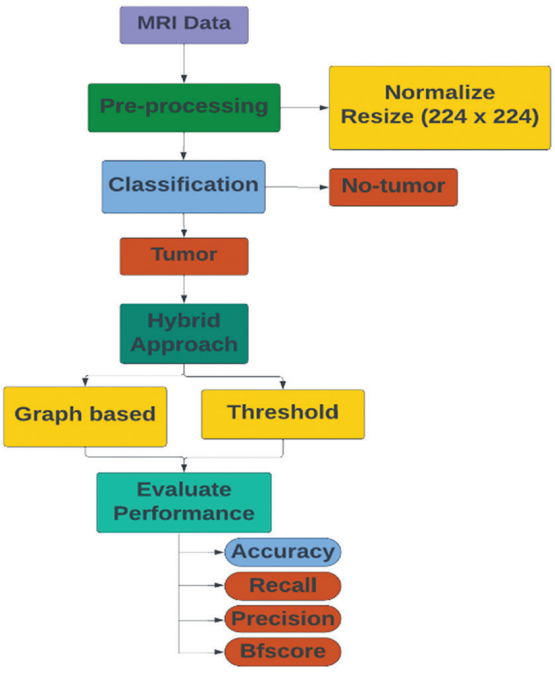

Fig. 2. Schematic representation of proposed system

4.1. DATASET SPECIFICATION

The dataset was obtained from distinct hospitals and encompasses three categories of brain tumor cases, namely atypical meningioma, glioma, and schwannoma, alongside normal brain images. Initially stored in the DICOM format, these images underwent preprocessing, during which they were converted into the JPG format. The collected dataset consists of various MRI sequences for further pre-processing. Following preprocessing, the images were categorized into two groups: with tumors and no-tumor, and facilitating further analysis. The dataset comprises a total of 884 MRI brain images categorized into two classes: 624 images with tumors and 260 images of normal brains. The brain MRI dataset is divided into training and test sets, with 707 images for training and 77 for testing. Each image has been resized to 224 x 224 pixels. A summary of the dataset specifications is provided in Table 1.

Table 1. Dataset specification

Data	Specification
Dataset source	Safdarjung, Medanta and SGPGI Hospitals
Image Format	DICOM
Size of Images	224 x 224
No. of Classes	Two
Name of Classes	Tumor, No-tumor
Name of Sequence	T1, T2, FLAIR, T1+C
Train	80%
Test	20%

In Table 2 the demographic details of patients with three brain tumor categories including atypical meningioma, glioma, and schwannoma, along with normal brain MRI images. The patient data has been collected from radiologists, accompanied by authorized reports and the consent of both patients and, their attendants.

Table 2. Demographic details of patients

Patient	Hospital	Age	Gender	Category
Patient#1	Medanta	58	Female	Glioma
Patient#2	SGPGI	54	Male	Schwannoma
Patient#3	Safdarjung	62	Female	Atypical Meningioma
Patient#4	SGPGI	45	Female	Normal brain

4.2. MRI IMAGING SEQUENCES

All MRI sequences exhibit diverse properties characteristics, and distinct appearances, which play a crucial role in the analysis and grading of tumors. These MR sequences rely on the application of radiofrequency pulses and gradients to capture detailed tissue information and intensity variations. For instance, FLAIR images are valuable for assessing lesions near the ventricles and distinguishing them from cerebral spinal fluid (CSF).

In the T2 sequence, which is often used in the evaluation of inflammatory processes, many diseases manifest an increase in tissue fluid content. Consequently, these lesions appear brighter and are employed, much like T1-weighted imaging, to assess anatomical structures and most lesions throughout the body. However, it is important to note that T2-weighted imaging may not be the optimal choice for evaluating lesions around the brain ventricles, as both lesions and CSF can have a similar appearance in this sequence.

On the other hand, T1-weighted images with contrast enhancement (T1+C), achieved by injecting contrast material like gadolinium, serve to increase the T1 signal from moving blood. These MRI sequences will be discussed in more detail in the context of the specific images used.

4.2.1. Fluid-Attenuated Inversion Recovery (FLAIR) image

The FLAIR image in MRI is notable for its similarities to T2-weighted imaging regarding brain tissue intensities, with the key distinction being the appearance of cerebrospinal fluid (CSF) as dark rather than bright. It achieves this by selectively suppressing the signals from fluids through the use of long echo (TE) and repetition (TR) times.

In FLAIR images, grey matter appears brighter than white matter, and CSF stands out as dark. This particular characteristic makes FLAIR sequences a valuable tool for the assessment of various brain disorders, including infarction, hemorrhage, and head traumas. Additionally, FLAIR imaging has the added benefit of reducing cerebrospinal fluid production. An illustrative example of the axial view of a FLAIR image is depicted in Fig. 3.

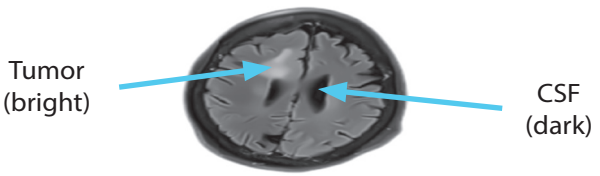

Fig. 3. Axial view of FLAIR sequence

4.2.2. T1 image

In the T1 sequence, tissue intensities reflect T1, which is the long relaxation time. On T1 scans, fatty tissue appears bright, but CSF with no fat appears dark. The T1 sequence produces short TE and TR times, which darkens the CSF. The axial view of the T1 image is represented in Fig. 4.

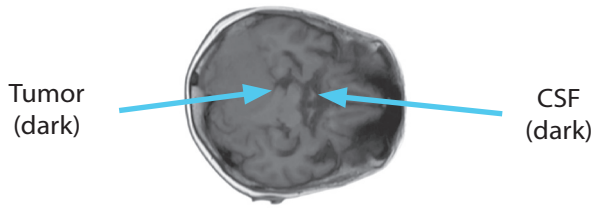

Fig. 4. Axial view of T1 sequence

4.2.3. T2 image

The T2-weighted sequences generate long TE and TR times, making CSF appear very bright. In the T2 sequence, fluid, bone, and air appear dark. As a part of the inflammatory process, most diseases exhibit increased fluid content, causing lesions to appear bright. The sagittal view of the T2 image is shown in Fig. 5.

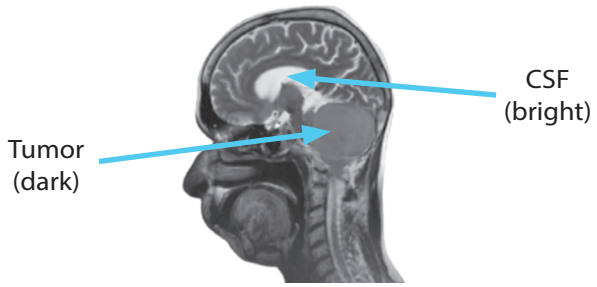

Fig. 5. Sagittal view of T2 sequence

4.2.4. T1+C image

In the T1+C sequence, contrast material is injected, which increases the T1 signal from moving blood and thus allows the detection of highly vascular lesions. Tissues have the same intensities as in T1, except that the moving blood is bright. It is useful in determining hypervascular lesions in haemangiomas and lymphangiomas. The axial view of the T1+C image is shown below in Fig. 6.

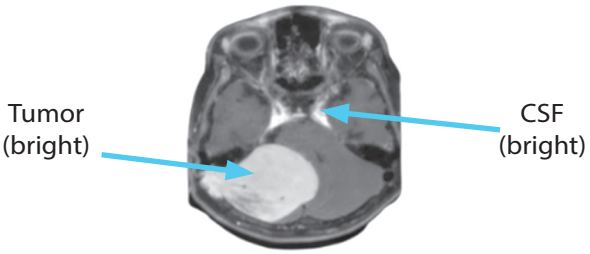

Fig. 6. Axial view of T1+C sequence

The properties of the MRI sequences are compared and represented in Table 3.

Table 3. Comparison between MRI sequences

MRI Sequence	CSF	White Matter	Grey Matter	TE/TR
T1	Hypointense	White	Grey	Short/Short
T2	Hyperintense	Grey	White	Long/Long
FLAIR	Hypointense	Grey	White	Very Long/ Very Long
T1+C	Hyperintense	White	White	Long/Long

The MRI scans can be viewed in three dimensions, namely Sagittal, Axial, and Coronal, allowing medical professionals to study the morphology of tumors as shown in Fig. 7.

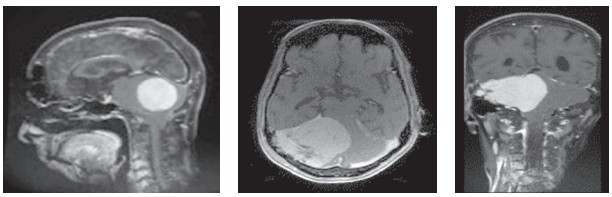

(a) (b) (c)

Fig. 7. (a) Sagittal (b) Axial, and (c) Coronal plane

4.3. CONVOLUTIONAL NEURAL NETWORK

The architecture of the CNN model is shown in Fig. 8. The deep learning process consists of 2D convolution and max-pooling layers.

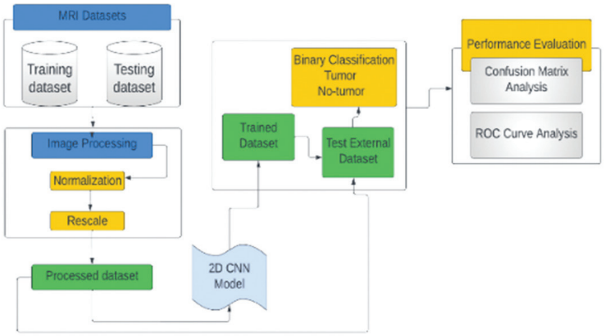

Fig. 8. Representation of 2D CNN Model

MRI datasets are utilized, encompassing training and validation approaches. The images undergo normalization and augmentation processes, and the processed dataset is then fed into the 2D model. Finally, the model produces binary classification results, which are used to categorize MRI brain images into tumor and no-tumor categories.

To improve the performance of the CNN model, the dataset has been normalized for feature scaling. The process begins with image pre-processing, which includes the augmentation of images. After that, data generators are created, and random patches extracted from MR images are inserted as input. The model has a total of 11 layers with varying numbers of neurons and dense layers such as convolution layers, batch normalization layers, max-pooling layers, and LeakyReLU layers. The process of convolution deep learning is processed with the SoftMax, and pixel classification layers. The architecture of CNN network layers is shown in Fig. 9.

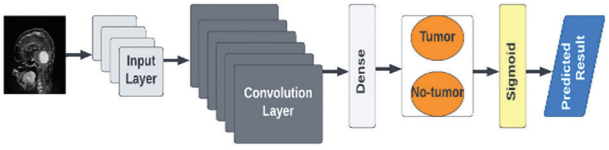

Fig. 9. Architecture of 2D CNN layers

The total number of layers can be counted as follows:

Input Layer: The model takes grayscale images with dimensions (150, 150, 1) as input.

Convolutional Blocks:

First Block: Applies Convolutional operation with 8 filters, kernel size (5, 5), and LeakyReLU activation. Followed by MaxPooling2D layer (2, 2).

Second Block: Applies Convolutional operation with 8 filters, kernel size (3, 3), and LeakyReLU activation. Followed by MaxPooling2D layer (2, 2).

Third Block: Applies Convolutional operation with 16 filters, kernel size (3, 3), and LeakyReLU activation.

Fourth Block: Applies Convolutional operation with 16 filters, kernel size (3, 3), and LeakyReLU activation. Followed by BatchNormalization for normalization and MaxPooling2D layer (2, 2).

Flatten Layer: Converts the 2D feature maps into a 1D vector.

Fully Connected Layers: Dense Layer (Hidden): Consists of 10 neurons with LeakyReLU activation.

Dense Layer (Output): Consists of 2 neurons with Softmax activation, representing the output classes for binary classification.

Optimizer and Compilation: Uses the Adam optimizer with a learning rate of 0.001, beta_1 of 0.9, and beta_2 of 0.999. Compiles the model with categorical crossentropy loss and accuracy as the metric.

Data Augmentation: Utilizes the ImageDataGenerator for real-time data augmentation during training.

Training Configuration: Specifies 100 epochs and a batch size of 40 for training. The architecture is shown in Fig. 10.

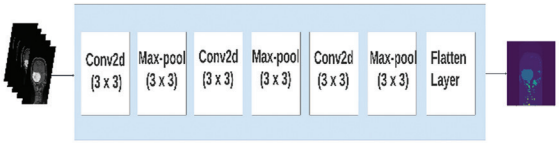

Fig. 10. CNN neural network layers

4.4. HYBRID APPROACH FOR SEGMENTATION

To locate tumors, a hybrid approach is applied. Firstly, graph-based segmentation is used, and thereafter, the threshold method is applied to the segmented MRI brain images.

4.4.1. Graph-based

Graph-based [19] method was originally introduced for a greedy approach to image segmentation based on predicates and has been utilized in various fields of image processing. The predicate P concludes in case there is an edge for segmentation. The fast minimum tree-based clustering on the image grid that produces a multichannel image is one of the concepts of graph-based segmentation concepts used in the proposed method and can be defined as:

$$P(a_1, a_2) = \begin{cases} \text{true} & \text{if } \text{Diff}(a_1, a_2) > \text{Dint}(a_1, a_2) \\ \text{false} & \text{otherwise} \end{cases}, \quad (1)$$

$P(a1, a2)$ is a binary indicator function in Eq. (1) that outputs true if the variation between modules $a1$ and $a2$, denoted by Diff($a1, a2$), is greater than the internal variation within $a1$ and $a2$, represented by Dint($a1, a2$). Otherwise, it outputs false.

$$\text{Diff}(a_1, a_2) = \min_{v_i \in a_1, v_j \in a_2, (v_i, v_j) \in E} w(v_i, v_j), \quad (2)$$

Diff($a1, a2$) in Eq. (2) represents the variation between two modules. It calculates the minimum weight edge connecting a node v_i in module $a1$ to a node v_j in $a2$.

The term $w(v_i, v_j)$ represents the weight associated with the edge connecting node v_i in module $a1$ to node v_j in module $a2$.

$$\text{Max}(a) = \max_{e \in \text{MST}(a,E)} w(e), \quad (3)$$

Max(a) in Eq (3), calculates the maximum weight edge in the Minimum Spanning Tree (MST) of the module a. $w(e)$ is a function that assigns a weight to the edge e in the graph.

$$\text{Dint}(a1, a2) = \min(\max(a1 + \tau(a1), \max(a2) + \tau(a2)), \quad (4)$$

Dint ($a1, a2$) in Eq. (4) calculates the internal variation within modules a1 and a2. It involves the minimum of the maximum weights of nodes in the modules with a threshold factor $\tau(a)$.

$$\tau(a) = \frac{k}{|a|}. \quad (5)$$

In eq. (5), k is a constant or parameter, and $|a|$ denotes the cardinality (number of elements) in the set a.

4.4.2. Threshold

The threshold method is a very simple technique used to select threshold value T. The RGB image is converted into a grayscale image, and further, it is converted into a binary image for a segment of the tumor region. The threshold value, T, is obtained from the grayscale image and is classified within the range of 0 to 255. The formula for the threshold can be given as in Eq. (6):

$$m(i, j) = \begin{cases} 0 & if\ k\ (i,\ j) < T \\ 1 & if\ k\ (i, j) \geq T \end{cases}, \quad (6)$$

where, $k\ (i, j)$ is an image and m (i, j) is grey conversion.

In Fig. 11, the proposed method has been combined to locate the tumor region. Further, the selected RGB image is scaled and segmented to partition affected tissue from MR brain images. In the final stage, morphological operation is applied.

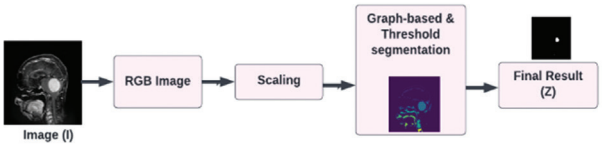

Fig. 11. Graph-based and threshold segmentation method

The hybrid approach algorithm is formed which is given as:

Start

[Step 1] Input MRI brain image (I) from datasets

[Step 2] Check for the presence of a tumor (Classification)

[Tumor Present]

[Step 3] Partition Image ($I1$, $I2$, ..., In)

[Step 4] Determine the number of partitions (n) using felzenswalb()

[Step 5] Cluster the Partition Images based on Image grid (k) [300 <= k <= 1000]

[Step 6] Set Parameters (S):

- Image (Height, Width), Scale: 350
- Sigma: 0.2, Min_Size: 20
- Threshold T >= 80

[Step 7] Compute the approximate distance (D_T) of Pixels of Tumors Image

[Step 8] Return the final segmentation result

[No Tumor]

[Step 9] Return the result "No Tumor Detected"

End

In the algorithm, select MRI brain images as input from the dataset for tumor segmentation. The input image is partitioned into 'n' numbers of segments using the Felzenszwalb() module. The partitioned image is clustered based on the image grid (k) with a range of 300 >= k <= 1000 and set parameters (S) for image (I) such as to scale indicate the largeness of clusters, sigma for smoothening of the image, min_size defines the size of the output image and set threshold T >= 80 for segmentation. After setting parameters, compute the approximate distance (D_T) of pixels of the tumor image. Finally, the result of Z is computed.

The observation result of testing images is shown in Fig. 12 column-wise.

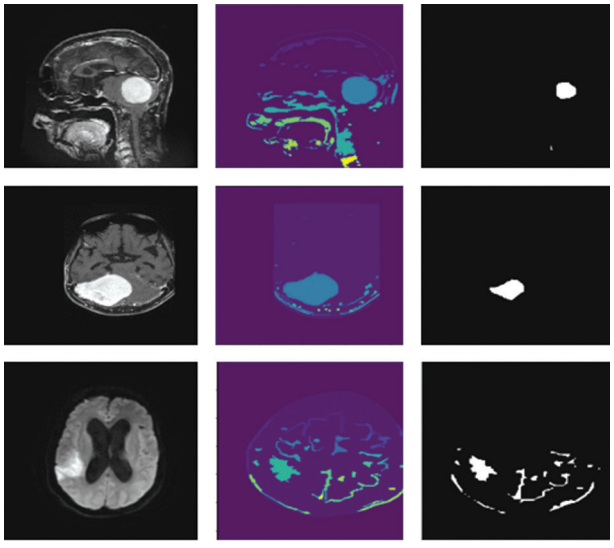

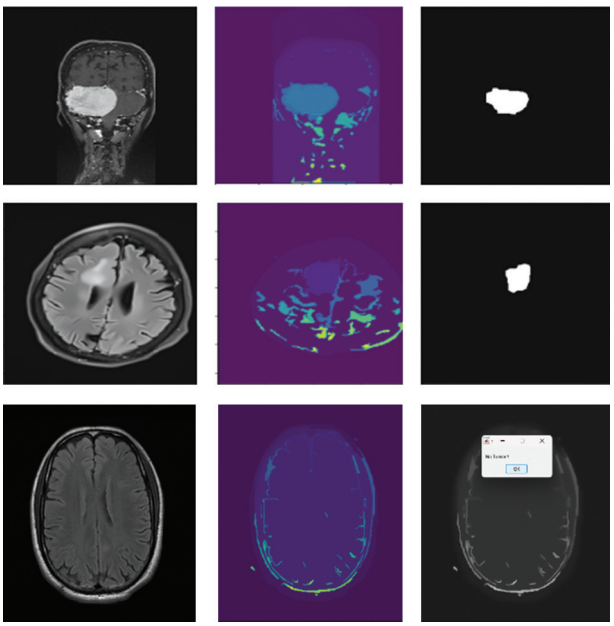

(a) (b) (c)

Fig. 12. Brain tumor segmentation using a hybrid approach: (a) Original images, (b) Graph-based segmentation, (c) Hybrid approach

5. EVALUATION METRICS AND RESULTS

The proposed method of classification and segmentation is implemented on a computer with an intel core i5 11th generation processor unit with 8GB RAM, operating at a frequency of 2.40 GHz, and NVIDIA GEFORCE GTX, using Python programming language. The results in the research work are discussed.

To calculate accuracy, a confusion matrix is created for classifying models and evaluating the segmentation outcomes of the proposed method.

$$\text{Accuracy} = \frac{(TP+TN)}{(TP+TN+FN+FP)}, \tag{7}$$

$$\text{Recall (r)} = \frac{TP}{(TP+FP)}, \tag{8}$$

$$\text{Precision (p)} = \frac{TP}{(TP+FP)}, \tag{9}$$

The confusion matrix includes True Positive (TP), True Negative (TN), False Positive (FP), and False Negative (FN), which are essential for assessing classification accuracy, recall, and precision. Additionally, BF (Boundary F1) score and Jaccard are employed to assess segmentation performance, as outlined in Eq. (7)-(11).

The BF score, a contour matching score, is utilized to evaluate image segmentation techniques. In this scenario, the two groups considered are the binary mask of objects and the segmentation result obtained from the hybrid approach.

$$\text{Bfscore (S (x, y), G (x, y)} = 2*\frac{p*r}{(r+p)}, \tag{10}$$

In the provided context, S (x, y) represents the input image, and G (x, y) is the binary mask depicting the seg-

mentation result. The variables r denote recall, and p signifies precision.

$$Jaccard(A, B) = |intersection(A, B)\ |/|\ union(A, B)|, \quad (11)$$

where A is the input image and B is the ground truth image.

5.1. RESULTS

5.1.1. Performance of classification

By examining the study depicted in Fig. 13 (a, b, c). It can be observed that the training accuracy acquired at 98.01% and the validation accuracy at 98%. The data was split into 80 % for training and 20% for validation.

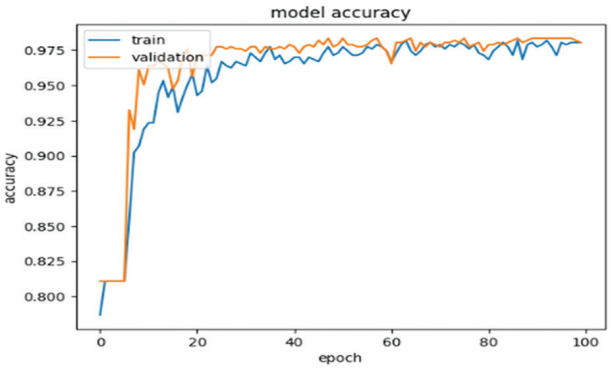

Fig. 13. (a) Training and validation accuracy

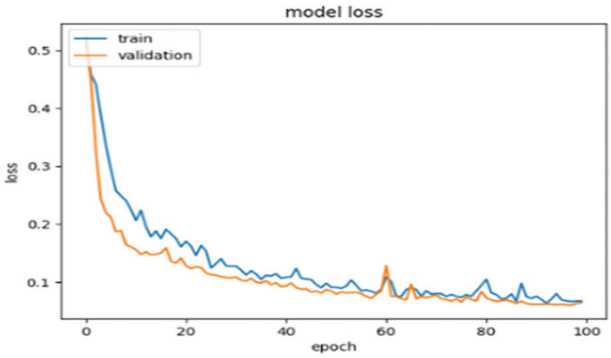

Fig. 13. (b) Training and validation loss

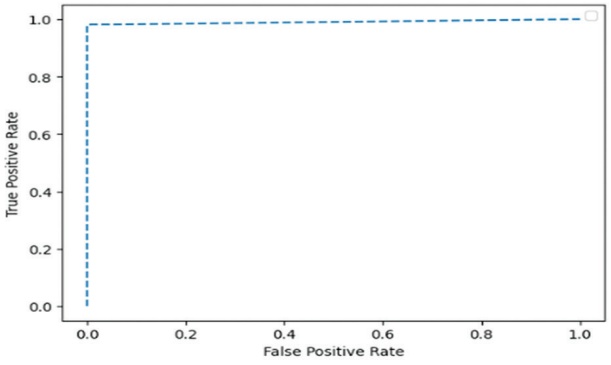

Fig. 13. (c) True Positive and False Positive Rate

The classification results of tumor and no-tumor are represented in Fig. 14.

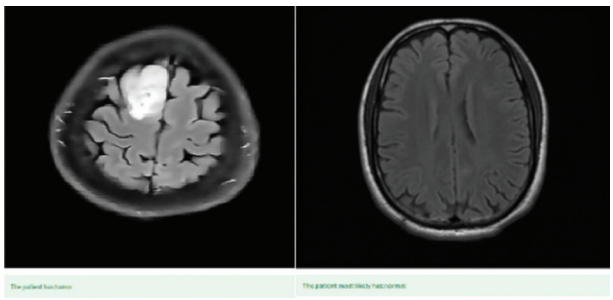

Fig. 14. Tumor and no-tumor classification results

5.1.2. Performance measure of segmentation

To assess and scrutinize the performance of the proposed hybrid method for tumor segmentation, a comparison is made with the ground truth image. Five images obtained are utilized as test images.

Table 4 shows results with Bfscore, and Jaccard, indicating the similarity coefficients and segmentation outcomes. The results for each test image demonstrate satisfactory performance.

Table 4. Results based on similarity coefficients (a) Original image, (b) Ground truth image, (c) Segmentation using a hybrid approach, (d) Bfscore, and (e) Jaccard

Input	Ground Truth	Hybrid approach	Bfscore	Jaccard
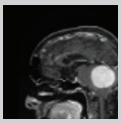	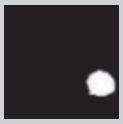		0.92236	0.88438
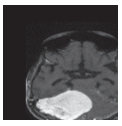			0.88353	0.88912
			0.56858	0.6722
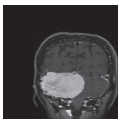			1	0.93862
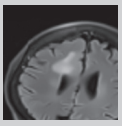			0.87662	0.72371
(a)	(b)	(c)	(d)	(e)

6. DISCUSSION

The successful performance of the proposed system and comparative results are summarized in Table 5.

According to Table 5, Zhang et al. [20] employed back propagation neural network (BPNN) classification following the enhancement of image quality using 2D DWT Decomposition. They achieved a classification accuracy of 98.10% but were limited to consist of T2-

weighted MR brain images, with only 66 images for training and testing. Notably, they did not incorporate any segmentation technique to locate tumor regions. Selvaraj et al. [21] achieved an accuracy of 96%, but they used a support vector machine classifier as a validation technique. Al Kadi et al. [22] focused on extracting histopathological features, without applying any segmentation method, and achieved an accuracy of 92% accuracy using a fuzzy clustering machine for classification. In contrast, Muezzinoglu et al. [23] proposed the ResNet50 transfer learning technique, classifying multiple types of brain tumors with a 98% accuracy. Georgiardis et al. [24] attained an accuracy of 93%, though segmentation was not part of their study. Considering the studies outlined in Table 5 it is evident that the proposed method in this paper boasts minimum computational complexity and demonstrates commendable segmentation accuracy.

The essential stages of the research are as follows:

- The utilization of multimodal MRI sequence images is considered for the classification model.
- Implementation of 2D CNN to showcase high classification proficiency.
- Achievement of 98.89% accuracy in the proposed classification.
- Application of a hybrid approach for comparing test image results.
- Evaluation of similarity coefficients to yield robust segmentation results, with Bfscore registering a high value of 1 and Jaccard with 93.86%.
- However, some drawbacks of our proposed method include:
- The need for more cases of brain tumor for comprehensive validation.
- Suboptimal performance of the segmentation method when applied to non-contrast MRI brain images.

Table 5. Performance comparison between the proposed method and previous work

Author	Total images	Classification method	Classifier	Segmentation	Accuracy	F1 Score	Recall	Precision
Zhang et al. [20]	66	2D-DWT level 3 decomposition, DWT	BPNN	NA	98.02%	x	X	x
Selvaraj et al. [21]	1100	GLCM-4	LS-SVM KNN	NA	96%	x	X	x
Al Kadi et al. [22]	320	Histopathological features	FCM	NA	92%	x	X	x
Muezzinoglu et al. [23]	3264	ResNet50	Multi feature selector and KNN	NA	98.10%	98.01%	98.15%	97.91
Georgiardis et al. [24]	67	Histogram 4, LCM-22, GRLM-10	LSFT-PNN	NA	93%, 83.33%	75.65%	79%	88%
Proposed Method	884	CNN	Binary	Graph-based and Threshold	98.89%	-	98.14%	98.43%

7. CONCLUSION AND FUTURE WORK

The proposed segmentation technique, the hybrid approach, aims to more accurately locate tumor regions while achieving high classification accuracy. The presented work utilized an MRI brain tumor dataset, achieving a notable 98.89% accuracy using a 2D CNN model. Segmentation similarity coefficients, including a Bfscore of 1 and a Jaccard coefficient of 93.86%, underscore the effectiveness of our approach in tumor detection and segmentation. This method offers a promising avenue for future research, with plans to expand the dataset, incorporate more samples, and explore additional techniques for enhancing brain tumor location and diagnosis.

8. REFERENCES

[1] S. Chang, “Brain Tumor: Introduction”, www.cancer.net/cancer-types/brain-tumor (accessed: 2023)

[2] U. Asim, E. Iqbal, A. Joshi, F. Akram, K. N. Choi, "Active Contour Model for Image Segmentation with Dilated Convolution Filter", IEEE Access, Vol. 9, 2021, pp. 168703-168714.

[3] D. Deb, S. Roy, “Brain tumor detection based on hybrid deep neural network in MRI by adaptive squirrel search optimization”, Multimedia Tools and Applications, Vol. 80, 2021, pp. 2621-2645.

[4] R. Ranjbarzadeh, K. A. Bagherian, G. S. Jafarzadeh et al. “Brain tumor segmentation based on deep learning and an attention mechanism using MRI multi-modalities brain images”, Scientific Reports, Vol. 11, 2021, p. 10930.

[5] M. U. Rehman, S. Cho, J. Kim, K. T. Chong. “Brain-Seg-Net: Brain Tumor MR Image Segmentation via Enhanced Encoder-Decoder Network”, Diagnostics, Vol. 11, 2021, p. 169.

[6] G. Karayegen, M. F. Aksahin, “Brain Tumor Prediction on MR Images with Semantic Segmentation by using Deep Learning Network and 3D Imaging

of Tumor Region", Biomedical Signal Processing and Control, Vol. 66, 2021, p. 102458.

[7] H. Saleem, A. R. Shahid, B. Raza, "Visual Interpretability in 3D Brain Tumor Segmentation Network", Computers in Biology and Medicine, Vol. 133, 2021, p. 104410.

[8] A. Khosravanian, M. Rahmanimanesh, P. Keshavarzi, S. Mozaffari, "Fast Level Set Method for Glioma Brain Tumor Segmentation based on Superpixel Fuzzy Clustering and lattice Boltzmann Method", Computer Methods, and Programs in Biomedicine, Vol. 198, 2021, p. 105809.

[9] Y. Zhang, Y. Lu, W. Chen, Y. Chang, H. Gu, B. Yu, "MSMANet: A Multi-scale Mesh Aggregation Network for Brain Tumor Segmentation", Applied Soft Computing, Vol. 110, 2021, pp. 1568-4946.

[10] X. Lei, X. Yu, J. Chi, Y. Wang, J. Zhang, C. Wu, "Brain Tumor Segmentation in MR Images using a Sparse Constrained Level Set Algorithm", Expert Systems with Applications, Vol. 168, 2020, p. 114262.

[11] N. V. Shree, T. N. R. Kumar, "Identification, and Classification of Brain Tumor MRI Images with Feature Extraction using DWT and Probabilistic Neural Network", Brain Informatics, Vol. 5, 2018, pp. 23-30.

[12] S. K. Mamatha, H. K. Krishnappa, N. Shalini, "Graph Theory Based Segmentation of Magnetic Resonance Images for Brain Tumor Detection", Pattern Recognition and Image Analysis, Vol. 32, 2022, pp. 153-161.

[13] T. Balamurugan, E. Gnanamanoharan, "Brain tumor segmentation, and classification using hybrid deep CNN with LuNetClassifier", Neural Computing and Applications, Vol. 35, 2023, pp. 4739-4753.

[14] A. Hossain, M. T. Islam, T. Rahman, M. E. H. Chowdhury, A. Tahir, S. Kiranyaz, K. Mat, G. K. Beng, M. S. Soliman, "Brain Tumor Segmentation and Classification from Sensor-Based Portable Microwave Brain Imaging System Using Lightweight Deep Learning Models", Biosensors, Vol. 13, No. 3, 2023, p. 302.

[15] P. S. Bidkar, R. Kumar, A. Ghosh, "Hybrid Adam Sewing Training Optimization Enabled Deep Learning for Brain Tumor Segmentation and Classification using MRI Images", Computer Methods in Biomechanics and Biomedical Engineering: Imaging & Visualization, Vol. 11, No. 5, 2023, pp. 1921-1936.

[16] A. S. Ansari, "Numerical Simulation and Development of Brain Tumor Segmentation and Classification of Brain Tumor Using Improved Support Vector Machine", International Journal of Intelligent Systems and Applications in Engineering, Vol. 11, No. 2s, 2023, pp. 35-44.

[17] Z. Ullah, M. U. Farooq, S. H. Lee, D. An, "A hybrid image enhancement based brain MRI images classification technique", Medical Hypotheses, Vol. 143, 2020, p. 109922.

[18] J. Amin, M. Sharif, N. Gul, M. Yasmin, S. A. Shad, "Brain tumor classification based on DWT fusion of MRI sequences using convolutional neural network", Pattern Recognition Letters, Vol. 129, 2020, pp. 115-122.

[19] P. F. Felzenszwalb, D. P. Huttenlocher, "Efficient Graph-Based Image Segmentation", International Journal of Computer Vision, Vol. 59, 2004, pp. 167-181.

[20] Y. Zhang, D. Zhengchao, W. Lenan, W. Shuihua, "A Hybrid Method for MRI Brain Image Classification", Expert Systems with Applications, Vol. 38, No. 8, 2011, pp. 10049-10053.

[21] H. Selvaraj, S. T. Selvi, D. Selvathi, L. Gewali, "Brain MRI Slices classification using Least Squares Support Vector Machine", International Journal of Intelligent Computing in Medical Sciences and Image Processing, Vol. 1, No. 1, 2007, pp. 21-33.

[22] O. Al-Kadi, "A Multiresolution Clinical Decision Support System based on Fractal Model Design for Classification of Histological Brain tumours", Comput Med Imaging Graph, Vol. 41, 2015, pp. 67-79.

[23] T. Muezzinoglu et al. "PatchResNet: Multiple Patch Division-Based Deep Feature Fusion Framework for Brain Tumor Classification Using MRI Images", Journal of Digital Imaging, Vol. 36, 2023, pp. 973-987.

[24] G. Pantelis, C. Dionisis, K. Ioannis, D. Antonis, K. C. George, S. Koralia, M. Menelaos, N. George, S. Ekaterini, "Improving Brain Tumor Characterization on MRI by Probabilistic Neural Networks and Non-Linear Transformation of Textural Features", Computer Methods and Programs in Biomedicine, Vol. 89, No. 1, 2008, pp. 24-32.